

# Phytochemical Profiling and In Vitro Anticancer Activity of Purified Flavonoids of *Andrographis glandulosa*



## Authors

Neeraja Cherukupalli<sup>1\*</sup>, Sudarshana Reddy Bhumireddy<sup>2,3\*</sup>,  
Subrahmanya Sarma V Akella<sup>4</sup>, Aaysha Sataniya<sup>5</sup>, Prabhakar Sripadi<sup>2,3</sup>,  
Venkateswara Rao Khareedu<sup>1</sup>, Dashavantha Reddy Vudem<sup>1</sup>

## Affiliations

- 1 Centre for Plant Molecular Biology, Osmania University, Hyderabad, India
  - 2 National Centre for Mass Spectrometry, CSIR-Indian Institute of Chemical Technology, Hyderabad, Telangana, India
  - 3 Academy of Scientific and Innovative Research, CSIR-Indian Institute of Chemical Technology, Hyderabad, Telangana, India
  - 4 Centre for NMR and Structural Chemistry, CSIR-Indian Institute of Chemical Technology, Uppal Road, Tarnaka, Hyderabad, India
  - 5 Chemical Biology Division, CSIR-Indian Institute of Chemical Technology, Uppal Road, Tarnaka, Hyderabad, India
- \* Contributed equally

## Key words

*Andrographis glandulosa*, Acanthaceae, chemical profiling, LC-MS, NMR-spectroscopy, ESI-MS/MS, anticancer activity

received 15.11.2016

revised 18.02.2017

accepted 28.02.2017

## Bibliography

DOI <http://dx.doi.org/10.1055/s-0043-105274>

Published online: 2017

Planta Med Int Open 2017; 4: e24–e34

© Georg Thieme Verlag KG Stuttgart · New York

ISSN 2509-9264

## Correspondence

Prof. V. Dashavantha Reddy

Centre for Plant Molecular Biology

Osmania University

Hyderabad 500007

India

Tel.: +91/40/27098 087, Fax: +91/40/27096 170

vdreddycpmb@yahoo.com

## ABSTRACT

The genus *Andrographis* includes diverse species of medicinal importance. The present study for the first time unravels the chemical profiling and medicinal importance of an unexplored species, *Andrographis glandulosa*. LC-MS analysis of *A. glandulosa* methanolic extract disclosed it as a rich source of flavonoids, with 8 minor peaks and 2 major peaks (*m/z* 285.0749 and 283.0595). NMR and ESI-MS/MS analyses confirmed the major peaks as (R) 2',5-dihydroxy-7-methoxyflavanone and 2',5-dihydroxy-7-methoxyflavone. Purified compounds exhibited antiproliferative activity on 3 cancer cell lines (HeLa, MIA PaCa and U-87) with IC<sub>50</sub> 39.81–46.21 μM for flavanone, and 20.84–25.16 μM for flavone. IC<sub>50</sub> values of flavone are on a par with that of the positive control quercetin (21.78–26.82 μM). HeLa cells treated with 117 μM flavanone showed a loss of MMP (~55 % of cells) resulting in apoptosis (~51 % of cells). Treatment with 80 μM flavone caused a loss of MMP (~88 % of cells) and induced apoptosis in ~70 % of cells proving its efficacy over flavanone. Purified flavonoids exhibited cytotoxicity by disrupting mitochondrial membrane, caspase 3 activation and apoptosis. Purified flavonoids appear as promising natural products for developing cancer therapeutics.

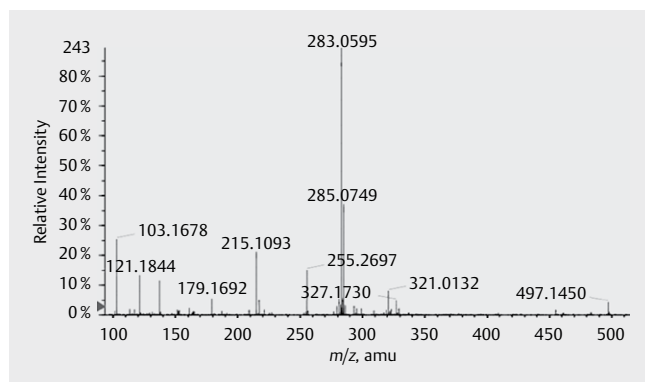
## Abbreviations

AGME	<i>Andrographis glandulosa</i> methanolic extract
HeLa	human cervical carcinoma cells
MIA	PaCapancreatic carcinoma
MMP	mitochondrial membrane potential
RDA	retro Diels-Alder reaction
U-87	glioblastoma

## Introduction

Cancer is a global problem with a large number of people being affected and the estimates indicate an increase of 70 % in cases by the end of next 2 decades [1]. Despite the availability of synthetic or semi-synthetic drugs, continued efforts are required to identify naturally occurring safe anticancer compounds that are free from side effects. Plants contributed more than 50 % of anticancer mol-

ecules that are being used in the treatment [2, 3]. The genus *Andrographis* belonging to the family Acanthaceae includes various species of medicinal importance and most of them are endemic to India. *Andrographis paniculata* (Burm.f.) Nees is well known and extensively studied at the molecular level [4, 5] for its various clinical applications and is being used widely in the preparation of Ayurveda, Siddha, and Unani medicines. The drug lead molecules such as andrographolide and neoandrographolide isolated from this plant exhibited potent anticancer properties [6–8]. Other species like *Andrographis lineata* Nees, *Andrographis nallamalayana* J.L.Ellis, *Andrographis serpyllifolia* (Vahl) Wight, etc. were reported to show antihyperlipidaemic [9], antipsoriatic [10], and anti-inflammatory [11] activities. However, *Andrographis glandulosa* Nees found in and around forests of the Cuddapah and Nellore districts of Andhra Pradesh, India, [12] is one of the species that remains unraveled for medicinal importance and chemical constituents.



► **Fig. 1** Negative ion ESI-MS spectrum of methanolic extract of *A. glandulosa*.

The focus on the discovery of plant-derived substances followed by biological screening, identification of therapeutic activity, mode of action, and relevant molecular targets led to the identification of potent anticancer molecules such as Vinca alkaloids, curcumin, taxol, etc. Usage of taxol for cancer treatment resulted in drug-resistance over a time period besides preventing mitotic spindle formation in healthy cells causing severe side effects [13, 14].

To overcome or minimize the negative effects of the treatment on normal cells, studies to identify novel plant based substances are essential. To date, few species from the genus *Andrographis* have been assigned with DNA barcodes [15] and exploited for their chemical constituents with various pharmacological activities. The present study, the first of its kind, focused on the profiling of secondary metabolites and determining the structure of major bioactive compounds in addition to evaluating their potential anticancer activity.

## Results and Discussion

The negative ion ESI-MS spectra of AGME, obtained from both instruments, consistently showed 2 major peaks appearing at  $m/z$  285.0749 (elemental composition of  $C_{16}H_{14}O_5$ ) and 283.0595 (elemental composition of  $C_{16}H_{12}O_5$ ; ► **Fig. 1**). The accurate mass values of these 2 major peaks, when subjected to metabolite search in online databases, such as Metlin (<http://metlin.scripps.edu/index.php>), The Human Metabolome Database (<http://www.hmdb.ca/spectra/ms/search>), and Metacyc (<http://metacyc.org/cpd-search.shtml>), revealed that these ions belong to deprotonated molecules,  $[M-H]^-$  of flavonoids. Similarly, plausible structures derived for all minor peaks are presented in ► **Table 1**. Accurate  $m/z$  values obtained in LC-MS analysis and classification of these metabolites using online database search revealed that AGME is rich in flavonoids consisting of both free aglycones and/or glycosidic conjugates.

LC-total ion current chromatograms (TICC) from triplicate runs consistently showed 2 major peaks at 18.87 and 25.07 min (► **Fig. 2**). The negative ion ESI spectrum of the peak eluted at 18.87 min showed an ion of  $m/z$  285, and the peak eluted at 25.07 min showed an ion of  $m/z$  283 which conformed to respective  $m/z$  values obtained from direct ESI-MS analyses. The 2 components were successfully isolated by preparative HPLC, and the compounds eluted at 18.87 and 25.07 min were labeled as compound **1** and compound **2**, respectively. The LC-MS analysis of the

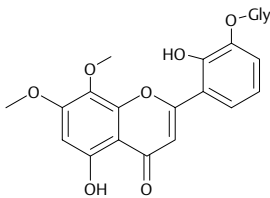
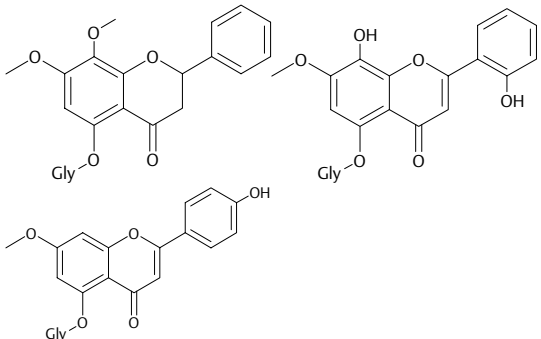
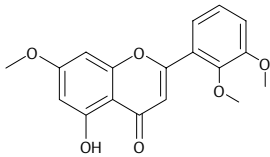
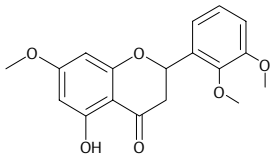
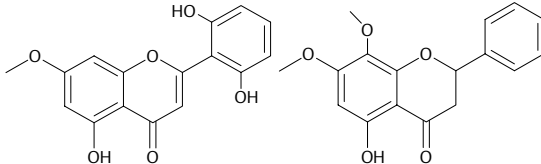
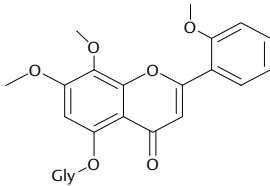
isolated compounds showed single peaks (data not shown). Purified compounds **1** and **2** with >95 % purity were analyzed by NMR and MS/MS techniques for elucidating their structures.

The  $^{13}C$  NMR spectrum of compound **1** displayed 16 carbon signals. The  $^1H$  NMR signals at  $\delta$  5.73 (1H, dd,  $J$  = 3.0, 12.9 Hz),  $\delta$  3.02 (dd,  $J$  = 12.09, 17.20 Hz) and  $\delta$  2.85 (dd,  $J$  = 3.0, 17.20 Hz) assigned to  $H_2$ ,  $H_3$ -axial, and  $H_3$ -equatorial, respectively, correspond to the flavanone basic skeleton. Coupling constant values between  $H_2$ ,  $H_3$ -axial, and  $H_3$ -equatorial revealed a stereochemistry at C-2 assigning R configuration.  $^{13}C$  NMR spectra recorded chemical shift values at  $\delta$  76.01 and 42.62 for  $C_2$  and  $C_3$ , respectively. 2 meta-coupled aromatic doublets (d,  $J$  = 2.3 Hz) at  $\delta$  6.06 and  $\delta$  6.11 for  $H_6$  ( $\delta_C$  94.89) and  $H_8$  ( $\delta_C$  95.74) showed the meta-substitution pattern on ring 'A'. A sharp singlet peak in the up field region at  $\delta$  3.82 (3H, s),  $\delta_C$  56.22 represents the presence of one methoxy group on ring 'A' at C-7 position. A set of 4 signals at  $\delta$  7.47 (dd, 1H,  $J$  = 7.5, 1.7 Hz),  $\delta$  7.17 (ddd, 1H,  $J$  = 7.5, 8.2, 1.7 Hz),  $\delta$  6.89 (ddd, 1H,  $J$  = 7.5, 7.5, 1.2) and  $\delta$  6.82 (1H, dd,  $J$  = 8.2, 1.2 Hz) correspond to 4 adjacent aromatic protons on ring 'C' and were assigned as  $H_6'$ ,  $H_4'$ ,  $H_5'$ , and  $H_3'$ , respectively. This data revealed a C-2' substituted ring 'C' and their corresponding  $^{13}C$  NMR analyses disclosed the chemical shift values at  $\delta$  116.14, 127.60, 130.33, and 120.62 (► **Table 2**). The UV absorption maximum at 281 nm revealed a flavanone basic skeleton. The above data assign the structure of compound **1** as 2',5-dihydroxy-7-methoxyflavanone (► **Fig. 3**).

The  $^{13}C$  NMR spectrum of compound **2** showed 16 carbon signals.  $^1H$  NMR spectrum showed one sharp 'singlet' at  $\delta$  7.24 (specific to flavones) without any further splitting ascribing as  $H_3$  proton on ring B, and its corresponding  $\delta_C$  at 111.10 ppm. 2 meta-coupled aromatic doublets (d,  $J$  = 2.3 Hz) at  $\delta$  6.67 and  $\delta$  6.36 for  $H_6$  ( $\delta_C$  94.4) and  $H_8$  ( $\delta_C$  99.76) showed the presence of meta-substitution pattern on ring 'A'. The spectrum also showed one sharp singlet peak in the up field region at  $\delta$  3.87 (3H, s),  $\delta_C$  57.89 corresponding to one methoxy group on ring 'A'. A set of 4 signals at  $\delta$  7.94 (dd, 1H,  $J$  = 8.0, 1.6 Hz),  $\delta$  7.34 (ddd, 1H,  $J$  = 8.3, 7.3, 1.6 Hz),  $\delta$  7.01 (ddd, 1H,  $J$  = 8.0, 7.3, 1.0), and  $\delta$  6.98 (1H, dd,  $J$  = 8.3, 1.0 Hz) revealed the presence of 4 adjacent aromatic protons on ring 'C' assigned to  $H_6'$ ,  $H_4'$ ,  $H_5'$  and  $H_3'$ , respectively, with corresponding  $^{13}C$  chemical shifts 118.77, 130.38, 134.90, and 121.29 (► **Table 2**). The UV absorption maxima at 210, 245, and 260 nm correspond to a typical flavone skeleton. The above data assign the structure of compound **2** as 2',5-dihydroxy-7-methoxyflavone (► **Fig. 3**).

Negative ion ESI mass spectrum of compound **1** showed a  $[M-H]^-$  ion at  $m/z$  285.07575 corresponding to the elemental composition  $C_{16}H_{14}O_5$ . The MS/MS spectrum of ion  $m/z$  285 recorded the product ions expected to be formed due to the fragmentation of flavanone aglycones (► **Fig. 4**). One prominent product ion appeared at  $m/z$  165 corresponding to the loss of  $C_8H_8O$  from  $[M-H]^-$  ion, representing a RDA reaction. The other RDA product ion leaving charge on substituted styrene part with  $m/z$  119 appeared with low abundance. These RDA product ions conform to the presence of hydroxy and methoxy substituents on ring 'A' and a hydroxy substituent on ring 'C' (► **Fig. 4**). Other product ions in the MS/MS spectrum of compound **1** which appeared at  $m/z$  270 and 242 correspond to the loss of  $CH_3$  and  $(CH_3 + CO)$  radical, respectively, from  $[M-H]^-$  ion. This fragmentation pattern supports the structure of the compound **1** as 2',5-dihydroxy-7-methoxyflavanone.

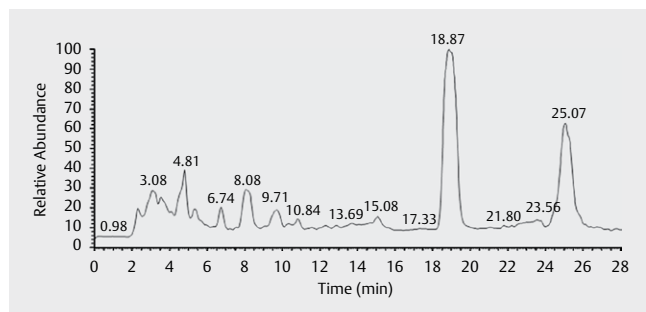
► **Table 1** Plausible structures of 8 minor peaks identified in LC-MS analysis.

S.No.	Accurate mass (m/z) of [M-H] <sup>-</sup>	Retention Time (min)	Category	Plausible structures
1	491.1206	2.92	Flavone-glycoside	
2	461.1098	3.19	Flavone-glycoside/ flavanone-glycoside	
3	327.2182	3.25	Flavone-glycoside	
4	503.1203	3.39		—
5	463.1256	3.94	Flavanone-glycoside	—
6	329.2338	3.99	Flavanone	
7	299.0565	7.02	Flavone-glycoside/ flavanone-glycoside	
8	489.1410	8.31	Flavone-glycoside	

Negative ion ESI mass spectrum of compound **2** showed the [M-H]<sup>-</sup> ion at m/z 283.0609 corresponding to the elemental composition C<sub>16</sub>H<sub>12</sub>O<sub>5</sub>. Comparison of MS data of compound **2** with that of compound **1** revealed an extra unsaturation (double bond) in compound **2**. MS/MS spectrum of ion m/z 283 showed the product ions characteristic of flavone aglycone (► **Fig. 5**). The major product ion at m/z 165 is the result of RDA reaction (► **Fig. 5**) and showed the presence of hydroxy and methoxy substituents in the ring 'A' (flavone structure). Other RDA product ion retaining charge on the

substituted ethynyl benzene which appeared at m/z 117 correspond to the molecular formula C<sub>8</sub>H<sub>6</sub>O. This ion provides the information about the presence of a hydroxyl group in ring 'C' with ethynyl phenol type of structure. Other products that appeared in the spectrum at m/z 268 (loss of CH<sub>3</sub>· from m/z 283), m/z 240 [loss of (CH<sub>3</sub> + CO)· from m/z 283] and m/z 121 correspond to the loss of CO<sub>2</sub> from m/z 165. This fragmentation pattern supports the structure of the compound **2** as 2',5-dihydroxy-7-methoxyflavone.

The antiproliferative activity of purified flavanone and flavone on 3 different cell lines is presented in ► **Fig. 6**. SRB assay results revealed varying  $IC_{50}$  values for purified compound **1** (m/z 285) on



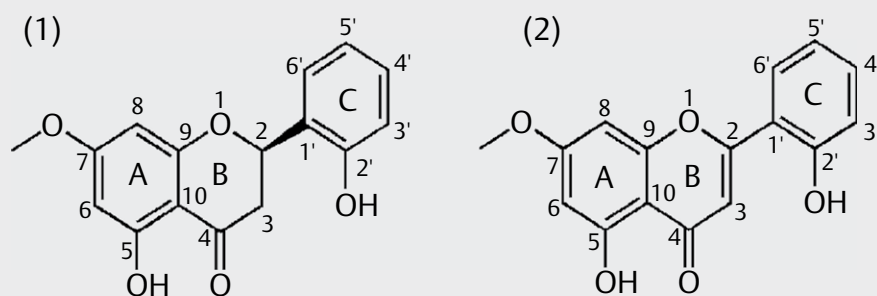
► **Fig. 2** Total ion chromatogram of methanolic extract of *A. glandulosa*. LC-MS of *A. glandulosa* showing 2 major peaks at 18.87 and 25.07 min of retention time with an m/z of 285 and 283, respectively.

HeLa (40.67  $\mu$ M), MIA PaCa (46.21  $\mu$ M), and U-87 (39.81  $\mu$ M) cells; whereas, compound **2** (m/z 283) exhibited higher antiproliferative activity with an  $IC_{50}$  of 20.84  $\mu$ M on HeLa, 24.36  $\mu$ M in MIA PaCa, and 25.16  $\mu$ M in U-87 cells. The positive control quercetin exhibited an  $IC_{50}$  of 25.16  $\mu$ M on HeLa, 26.82  $\mu$ M in MIA PaCa, and 21.78  $\mu$ M in U-87 cells. Both the aglycones viz., 2',5-dihydroxy-7-methoxyflavanone (m/z 285) and 2',5-dihydroxy-7-methoxyflavone (m/z 283), purified from *A. glandulosa*, exhibited antiproliferative activity in a dose-dependent manner.

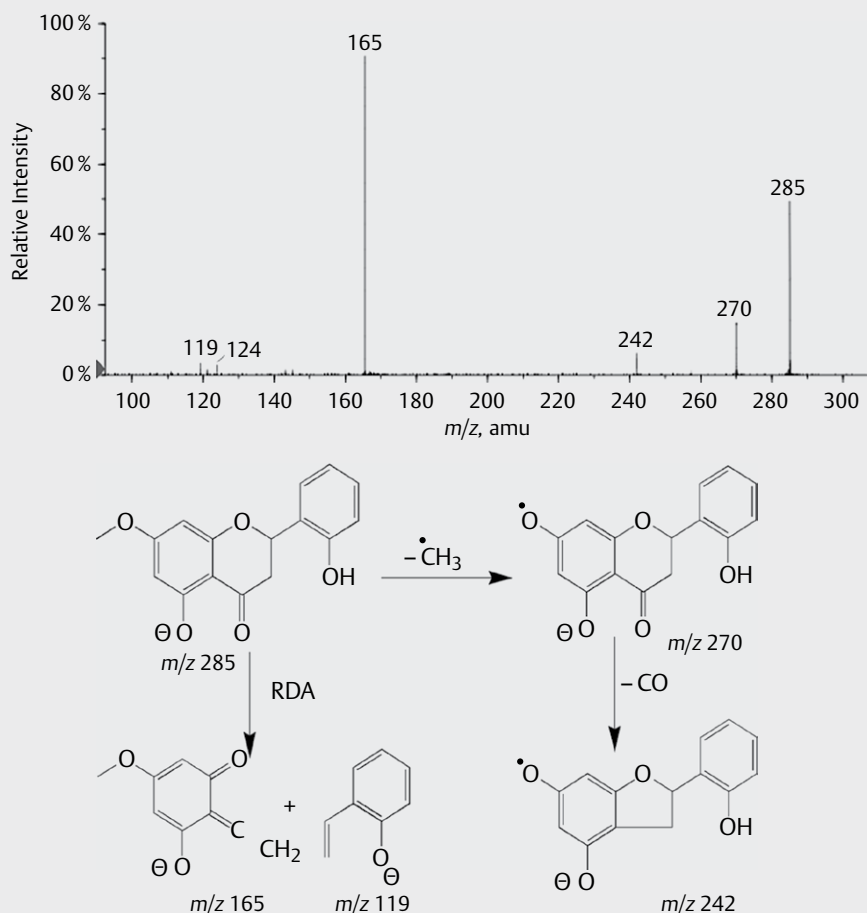
Flavonoids are polyphenolic compounds which are known to exhibit a wide range of pharmacological activities and are considered as prospective compounds for cancer therapy [16]. A considerable number of in vitro and in vivo studies have been carried out using natural flavonoids to establish the correlation between the flavonoid structure and their activity. In an earlier study, the flavonoids apigenin and chrysin having flavone basic skeletons exhibited potent anticancer activity. Apigenin was found to be effective in multiple ways, by inhibiting protein kinase C, phosphatidylinositol

► **Table 2**  $^1\text{H}$ NMR and  $^{13}\text{C}$ NMR derived chemical shift values of the 2 purified compounds.

Position	Compound 1 (RT 19 min and m/z 285)			Compound 2 (RT 25 min and m/z 283)		
	$^1\text{H}$ NMR ( $\text{CD}_3\text{OD}$ ) $\delta_{\text{H}}$ ppm	J (Hz)	$^{13}\text{C}$ NMR $\delta_{\text{C}}$ ppm	$^1\text{H}$ NMR ( $\text{CD}_3\text{OD}$ ) $\delta_{\text{H}}$ ppm	J (Hz)	$^{13}\text{C}$ NMR $\delta_{\text{C}}$ ppm
2	5.73	3.00, 12.9	76.01			159.3
3	ax 3.02	12.9, 17.2	42.62	7.24		111.1
	eq 2.85	3.00, 17.2				
4			188.8			178.3
5			158.9			149.5
6	6.11	2.3	94.89	6.67	2.2	94.4
7			164.3			151.6
8	6.06	2.3	95.74	6.36	2.2	99.76
9			164.5			146.2
10			106.3			109.5
1'			124.6			117.1
2'			153.6			156.7
3'	6.82	8.2, 1.2	116.14	6.98	8.3, 1.00	118.77
4'	7.17	7.5, 8.2, 1.7	130.33	7.34	8.3, 7.3, 1.6	134.9
5'	6.89	7.5, 7.5, 1.2	120.62	7.01	8, 7.3, 1.00	121.29
6'	7.47	7.5, 1.7	127.6	7.94	8, 1.6	130.38
OCH <sub>3</sub> -7	3.82		56.22	3.87		57.89
OH-5	10.74			10.71		
OH-2'	9.31			9.29		



► **Fig. 3** Molecular structure of the 2 purified compounds obtained at an RT 18.87 and 25.07 min. Compound **1**: 2', 5-dihydroxy-7-methoxyflavanone; Compound **2**: 2', 5-dihydroxy-7-methoxyflavone.

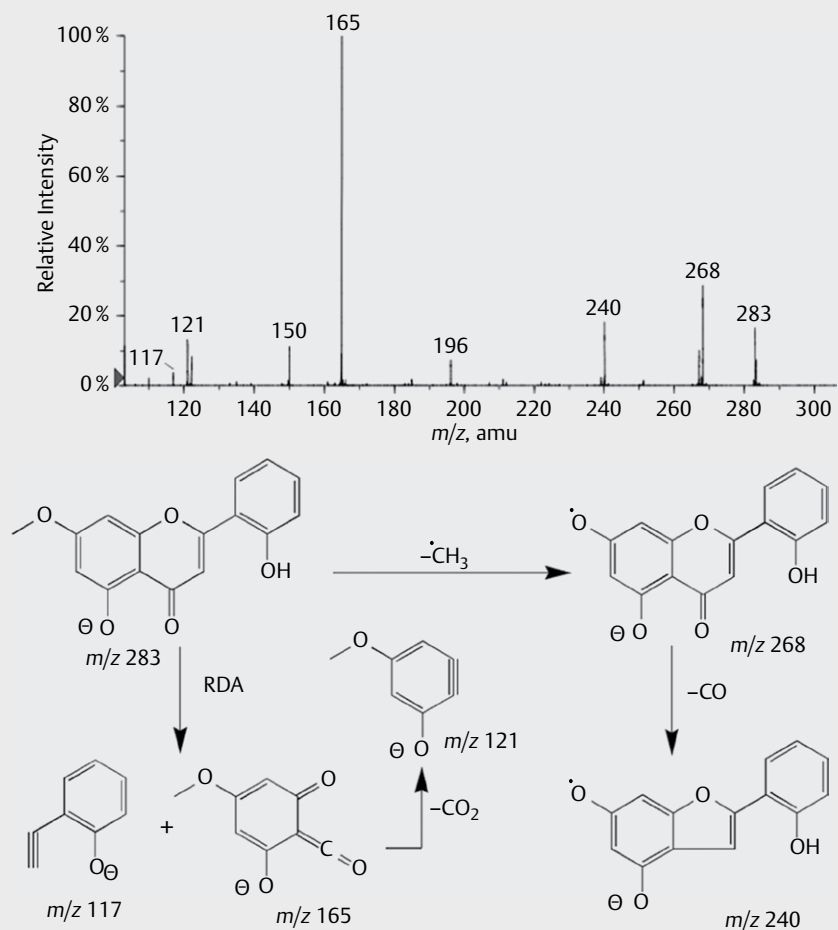


► **Fig. 4** ESI-MS/MS spectrum of the  $m/z$  285  $[M-H]^-$  ion. Scheme shows its CID mass fragmentation pattern.

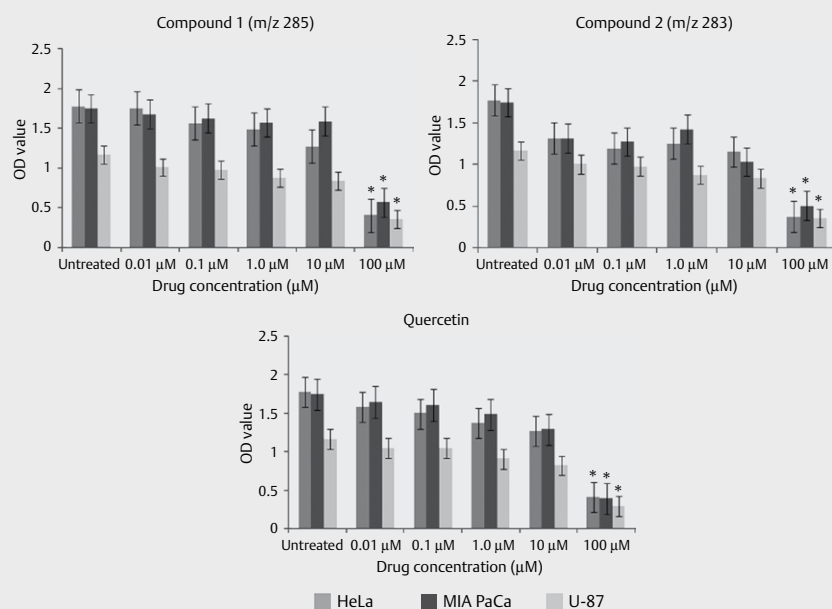
3-kinase (PI 3-kinase  $\alpha$ ) and also by blocking of the cell cycle at G2/M phase; whereas, chrysin was found effective in inhibiting topoisomerase II activity [17]. Similarly, another flavone, luteolin, was found to inhibit growth of HAK-1B hepatoma cells in xenografted mice by targeting signal transducer and activator of transcription 3 gene (STAT 3) by either ubiquitin dependent degradation in Tyr<sup>705</sup>-phosphorylated STAT3 and/or by down-regulation in Ser<sup>727</sup>-phosphorylated STAT3 through inactivation of CDK5, triggering apoptosis via up-regulation of Fas/CD95 [18]. Flavonoids are known to inhibit the action of CYP450s involved in the metabolic activation of procarcinogens and are also known to activate the enzymes like UDP-glucuronyl transferase, quinone reductase, and glutathione-S-transferase that are involved in detoxification and elimination of carcinogens [19]. A wide diversity in the structural patterns of flavonoids with varied targets provides a greater opportunity for identifying effective pharmacophores with potential anticancer properties. Flavonoids isolated from medicinal plants such as *Andrographis lineata* Nees [20], *Cassia tora* L. (Leguminosae) [21], and *Glycyrrhiza inflata* Batalin (Leguminosae) [22] exhibited potent anticancer activity. Flavonoids were found effective in inducing apoptosis, [23] arresting cell cycle by disrupting the mitotic spindle formation [24], and inhibiting angiogenesis [25, 26] in various cancers. In another study, a herbal formulation (Shemam-ruthaa) rich in flavonoid content was found effective in inhibiting

the proliferation of breast cancer cells [27]. Flavonoids such as quercetin, luteolin and 3-O-methylquercetin, isolated from *Achyrocline satureioides* (Lam.) DC. (Compositae), were found promising for cancer therapy [28].

Effects of purified compounds on MMP and apoptosis are presented in ► **Table 3**. HeLa cells treated with 57 or 117  $\mu M$  of the purified compound **1** (2', 5-dihydroxy-7-methoxyflavanone) (► **Fig. 7**) showed a loss of MMP in 26.5% (► **Fig. 7c**) or 54.8% of cells (► **Fig. 7d**) and the cells treated with 40 or 80  $\mu M$  of the purified compound **2** (2', 5-dihydroxy-7-methoxyflavone) exhibited a loss of MMP in 34.1% (► **Fig. 7e**) and 87.7% of cells (► **Fig. 7f**). The cells treated with 50  $\mu M$  of the positive control quercetin showed a loss of MMP in 24.3% of cells (► **Fig. 7b**). Similarly, the cells treated with 57 or 117  $\mu M$  of the purified compound **1** (► **Fig. 8**) resulted in 14% (► **Fig. 8c**) or 50.6% (► **Fig. 8d**) of apoptotic cells and the cells treated with 40 or 80  $\mu M$  of the purified compound **2** resulted in 30.4% (► **Fig. 8e**) or 69.6% (► **Fig. 8f**) of apoptotic cells. The cells treated with the positive control quercetin showed apoptosis in 32.5% of cells (► **Fig. 8b**). Apoptosis is a genetically programmed mechanism that can be induced through several molecular pathways. Mitochondria were found to play a key role in the process of apoptosis [29]. It was reported that prior to the common signs of nuclear apoptosis such as chromatin condensation and endonuclease-mediated DNA fragmentation, the cells exhibit reduction in the MMP



► **Fig. 5** ESI-MS/MS spectrum of the  $m/z$  283  $[\text{M}-\text{H}]^-$  ion. Scheme shows its CID mass fragmentation pattern.

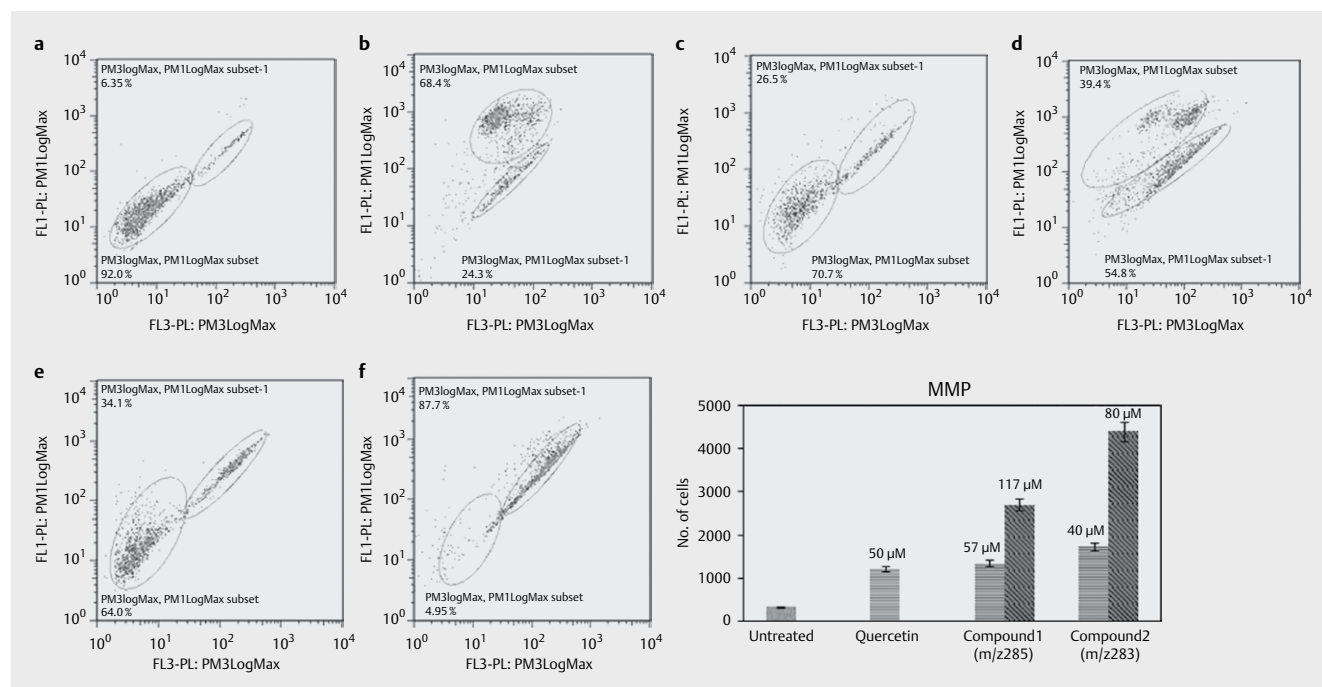


► **Fig. 6** Antiproliferative activity of purified flavonoids on 3 cancer cell lines. Treatment with different concentrations of purified flavonoids and standard compound quercetin. \*  $p$  value  $< 0.01$  was considered to be statistically significant (data is average of 3 replicates).

► **Table 3** Treatment of HeLa cells with purified flavonoids induced mitochondrial membrane depolarization and apoptosis.

	Compound 1 (m/z 285)		Compound 2 (m/z 283)		Untreated	Quercetin
Concentration ( $\mu\text{M}$ )	57	117	40	80	–	50
MMP	$1\,342 \pm 17^*$	$2\,694 \pm 46^*$	$1\,712.5 \pm 7.5^*$	$4\,388 \pm 3^*$	$320 \pm 1.5$	$1\,215 \pm 3.5^*$
APOPTOSIS	$690 \pm 10^*$	$2\,528 \pm 2^*$	$1\,516 \pm 4^*$	$3\,467 \pm 13^*$	$226 \pm 3$	$1\,625 \pm 7.07^*$

Mean number of cells (mean  $\pm$  SEM) showing mitochondrial depolarization/apoptosis (data is average of 3 replicates); \* p value < 0.01 was considered to be statistically significant

► **Fig. 7** Effect of the purified flavonoids on MMP in HeLa cells. Depolarized cells dispersed towards PM3 log max **a**. Untreated control showing 6.35% of depolarized cells **b**. Cells treated with 50  $\mu\text{M}$  of positive control Quercetin showing 24.3% depolarized cells **c, d**. Cells treated with 57  $\mu\text{M}$  or 117  $\mu\text{M}$  of 2', 5-dihydroxy-7-methoxyflavanone showing 26.5% or 54.8% depolarized cells **e, f**. Cells treated with 40  $\mu\text{M}$  or 80  $\mu\text{M}$  of 2', 5-dihydroxy-7-methoxyflavone showing 34.1% or 87.7% of depolarized cells.

leading to the opening of mitochondrial permeability transition pores [30]. It was also shown that mitochondrial depolarization occurs by the release of cytochrome c from the mitochondria into the cytosol which forms an essential part of the apoptosome [31, 32]. Of the 2 compounds studied, flavone revealed a higher anticancer activity compared to that of flavanone owing to its potential resonance, efficient electron delocalization and its stable flat structure.

To understand the mechanism involved in apoptosis, activation of caspase 3 was evaluated by Western blotting. As compared to untreated HeLa cells, treatment with 50  $\mu\text{M}$  of purified flavonoids for 24 h showed a drastic increase in the cleaved caspase 3 (► **Fig. 9**). Purified flavonoids caused a loss of mitochondrial membrane potential and this change in membrane permeability results in the release of specific proteins such as cytochrome c responsible for the activation of caspase 9 which in turn cleaves zymogen procaspase 3 into p17 and p12. The oligomerizations of these cleaved subunits are known to result in the formation of active executioner caspase 3. Tetrameric active caspase 3 is known to cleave proteins such as caspase 2, caspase 6, nuclear lamin, nuclear-DNA-dependent protein kinase, and DNA fragmentation factor 45 responsible for ap-

optosis [33, 34]. In conclusion, this study, the first of its kind, unravels the medicinal importance of *A. glandulosa* as it is a rich source of bioactive flavonoids and the 2 purified flavonoids seem promising for the development of therapeutic formulations for treating cancer.

## Materials and Methods

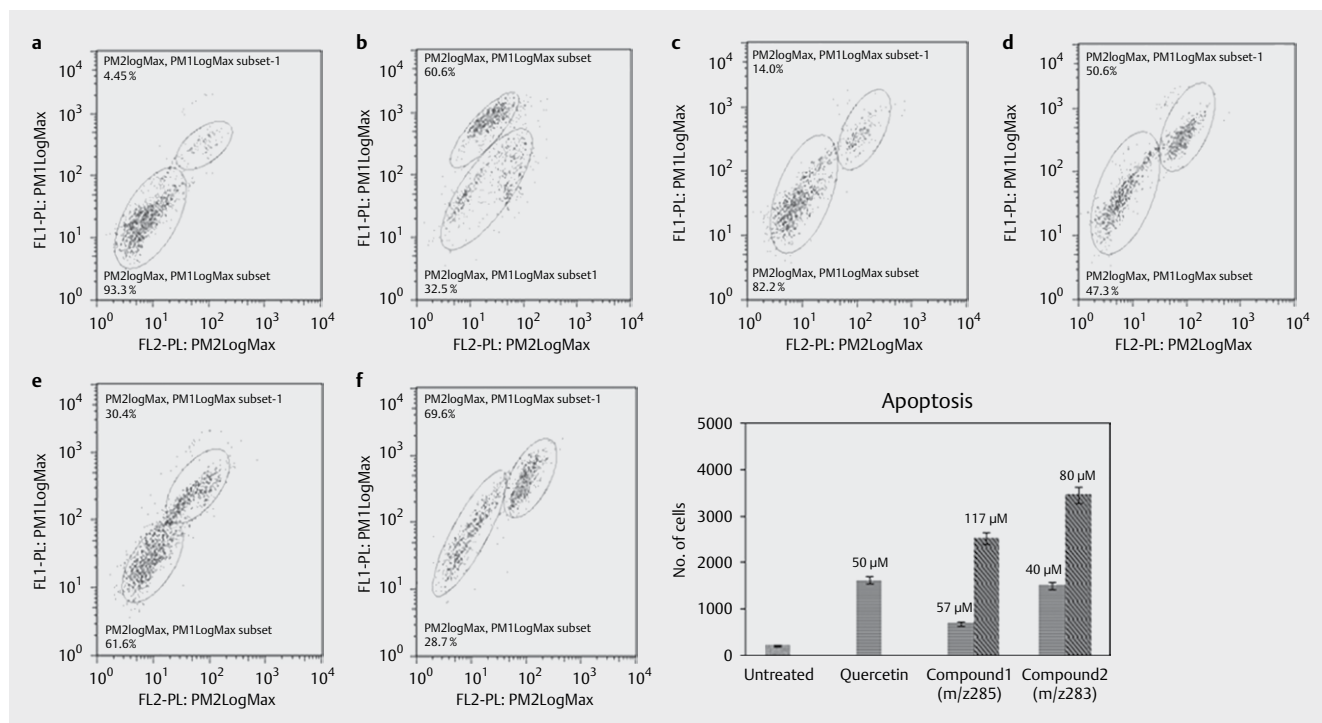
### Ethics statement

Plants used in the present investigation are neither endangered nor protected species and specimens were collected from open areas not requiring any permits.

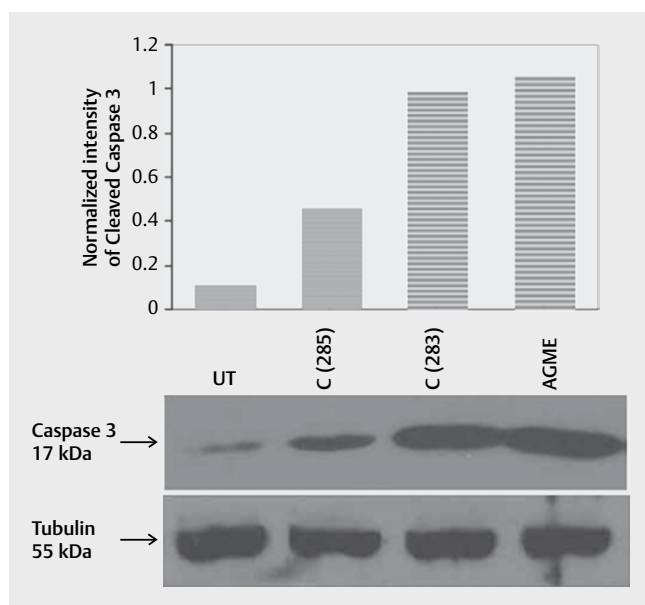
### Preparation of plant extracts

Plants of *A. glandulosa* (voucher id: CNS04AG2013) were collected from the Cuddapah district. Identification of the species was done based on the taxonomic literature and authentication given by Decan Circle, Botanical Survey of India. The plant materials were shade dried and cut into small pieces. The dried material (10 g) has been





► **Fig. 8** Effect of the purified flavonoids on apoptosis in HeLa cells. Apoptotic cells dispersed towards PM2 log max **a**. Untreated control showing 4.45% of the apoptotic cells **b**. Cells treated with 50  $\mu$ M of positive control Quercetin showing 32.5% of apoptotic cells **c**, **d**. Cells treated with 57  $\mu$ M or 117  $\mu$ M of 2', 5-dihydroxy-7-methoxyflavanone showing 14% or 50.6% of apoptotic cells **e**, **f**. Cells treated with 40  $\mu$ M or 80  $\mu$ M of 2', 5-dihydroxy-7-methoxyflavone showing 30.4% or 69.6% of apoptotic cells.



► **Fig. 9** Immunoblot of cleaved caspase 3 in lysates of HeLa cells treated with purified flavonoids. UT: Untreated control; C(285): Compound 1 (50  $\mu$ M); C(283): Compound 2 (50  $\mu$ M); AGME: methanolic extract of *A. glandulosa* (100  $\mu$ g).

ground into fine powder and subjected to soxhlet extraction in 300 mL of 100% methanol (Merck) at 65 °C. The resulting extract (AGME) was filtered using whatman filter paper and vacuum dried to remove trace amounts of methanol, if any.

### Sample preparation for metabolite analysis

Methanol (1 mL) was added to the dried crude extract (2 mg), vortexed for 5 min and the resulting solution was centrifuged for 5 min at 10 000 rpm. The supernatant was transferred into another fresh vial and concentrated to 500  $\mu$ L using Scanvac. The resulting solution was either immediately subjected for mass spectrometry analysis or stored in the refrigerator (4 °C) until further analyses.

### Direct ESI-MS and ESI-MS/MS analyses

Direct ESI-MS analyses were performed on a high resolution Q-TOF mass spectrometer (Q-Star XL, Applied Biosystems). Prior to sample analysis, methanol was injected into ESI-MS as solvent blank to rule out the background peaks. The spectral data was processed using Analyst software. Methanol was used as a mobile phase with a flow rate of 30  $\mu$ L/min and the samples were introduced into the source by the flow injection mode. Typical ESI conditions like 5.00 kV capillary voltage, 60 V declustering potential, 220 V focusing potential, 10 000 FWHM (Full Width at Half Maximum) as instrument resolution were employed. Analyses were carried out in triplicates under similar experimental conditions.

For ESI-MS/MS analyses the precursor ion of interest was selected using the quadrupole analyzer, collisions were made with nitrogen gas in the collision cell and resulted product ions were analyzed by TOF analyzer. Spectra were recorded using a collision energy of 30 eV.

### LC-MS and LC-photodiode array analyses

LC-MS and LC-photodiode array (PDA) analyses were performed on an Exactive Orbitrap mass spectrometer (Thermo Scientific) cou-



pled with a Thermo Accela 600 UHPLC pump and an Accela autosampler (Thermo Scientific). The chromatographic separation was achieved on a Zorbax Eclipse Plus C18 column (4.6 × 150 mm, 3.5 µm; Agilent). 2-component mobile phase consisting of methanol and water in 65:35 (v/v) composition was employed under isocratic mode with a run time of 28 min. Injection volume and flow rates were 8 µL and 0.6 mL/min, respectively, while the column temperature was maintained at 25 °C. For MS analysis, the LC eluents were allowed to enter into a heated electrospray ionization (HESI) probe with typical operational conditions of 300 °C probe temperature, 280 °C capillary temperature, 85 V capillary voltage, 4.5 kV spray voltage, and 175 V tube lens voltage. Nitrogen was used as both auxiliary and sheath gas at a flow rate of 45 and 15 mL/min, respectively. Mass range *m/z* 100 to 1 000 and resolution of 40 000 (FWHM) was employed. For LC-PDA analyses, the LC eluents were allowed to enter a Photo Diode Array detector (Accela PDA, 80 Hz) operated at the range of ultraviolet-visible wavelength (200 nm to 600 nm) using Deuterium and Tungsten lamps. Data was acquired using Xcalibur software (Thermo Scientific).

### Isolation of major compounds by preparative HPLC

The purification of both compounds corresponding to the 2 major peaks was carried out on a preparative HPLC (Waters) equipped with E0860F quaternary pump and PDA detector. Column specifications and mobile phase composition were same as mentioned in LC-PDA analysis. Dried methanolic extract of 100 mg was dissolved in 4 mL of pure methanol. A sample of 10 µL was injected and run for 30 min. To get a sufficient amount of each compound the experiment was repeated. At each run the first fraction was collected from retention time (RT) of 18.50 to 19.50 min, while the second fraction was collected from RT of 24.50 to 25.50 min. All the fractions collected for specific RT were pooled up in a round bottom flask. Rotary evaporation was done to get the compounds in a solid form free of solvent. The purity of the isolated compounds was authenticated by LC-MS analyses. The pure compounds were subjected to NMR, MS/MS analyses for structure determination and further evaluated for the anticancer activity.

### NMR analyses

NMR analyses were performed on AV-III 500 and AV-II 600 MHz NMR spectrometers at room temperature using the compounds dissolved in Methanol-D<sub>4</sub> (CD<sub>3</sub>OD) solvent. Residual methyl signal of solvent was used as internal reference. All the chemical shifts were measured in a 1D NMR (<sup>1</sup>H & <sup>13</sup>C NMR) spectrum and coupling constants were measured with resolution enhanced 1D spectrum. Chemical shift correlations were done using <sup>1</sup>H-<sup>1</sup>H double quantum filtered correlation (DQFCOSY) and <sup>1</sup>H-<sup>13</sup>C HSQC/HMBC spectra. These 2D spectra were processed with a Gaussian apodization in both dimensions.

### SRB assay of purified flavonoids

The cell lines, HeLa (doubling time: 19 h), MIA PaCa (doubling time: 40 h), and U-87 (doubling time: 34 h) used in this study were procured from American Type Culture Collection (ATCC). Purified flavonoids and quercetin, as positive control, (Sigma #Q4951, ≥95 % purity) were evaluated for their in vitro anti-proliferative activity. Sulforhodamine B (SRB) cell proliferation assay was used to estimate

cell viability after treating the cells with purified compounds for 48 h. All cell lines were grown in DMEM (containing 10 % FBS) in a humidified atmosphere of 5 % CO<sub>2</sub> at 37 °C. Cells cultured in T25 flasks were trypsinized after attaining subconfluent stage and seeded in 96-well plates in 100 µL aliquots at plating densities depending on the doubling time of individual cell lines. The microtiter plates were incubated at 37 °C, 5 % CO<sub>2</sub>, 95 % air and 100 % relative humidity. After 24 h of incubation, purified compounds with different concentrations (0.01, 0.1, 1, 10, and 100 mM) were added and incubated for 48 h. After 48 h of incubation at 37 °C, cell monolayers were fixed by the addition of 10 % (wt/vol) cold trichloroacetic acid and incubated at 4 °C for 1 h and were stained with 0.057 % SRB dissolved in 1 % acetic acid for 30 min at room temperature. Unbound SRB was washed with 1 % acetic acid. The protein-bound dye was dissolved in 10 mM Tris base solution and OD was measured at 510 nm using a microplate reader (Enspire, Perkin Elmer).

### Analysis of flavonoid-induced mitochondrial membrane depolarization and apoptosis by flow cytometry

HeLa cells were cultured for 24 h in 12 well plates (3 × 10<sup>4</sup> cells/mL) and treated with 57 µM/117 µM of compound **1** or 40 µM/80 µM of compound **2** for 24 h. Quercetin (50 µM) was used as positive control. Media were removed from each well and washed with 1X PBS. Cells were trypsinized with 0.125 % Trypsin EDTA (Himedia #TCL042) for one minute and the cell pellet was collected by centrifugation at 300 × *g* for 2 min. Cells were resuspended in 6 mL of complete culture medium and the cell concentration was maintained at 2 × 10<sup>4</sup> cells/mL. From this 200 µL of cells were aliquoted into 1.5 mL eppendorf tubes and following the manufacturer's protocol, changes in the mitochondrial membrane potential (MMP) and percentage of apoptosis were determined by flow cytometry using Guava® EasyCyte™ MitoPotential™ Kit (Cat. No. 4500-0250) consisting of 2 dyes JC1 and 7-amino actinomycin D (7AAD). For each treatment data was acquired for 5 000 cells.

### Western blotting

HeLa cells were seeded in 6-well plates at 0.2 million cells per well in DMEM (containing 10 % FBS) and incubated in a humidified atmosphere of 5 % CO<sub>2</sub> at 37 °C. After 24 h of incubation the cells were treated with 50 µM of either of purified flavonoids or 100 µg of crude methanolic extract for 24 h. Cells were washed with 1X PBS and subsequently whole cell lysates were prepared in 150 µL of 1 × sample buffer (180 mM Tris-Cl pH 6.8, 6 % SDS, 15 % glycerol, 7.5 % β-mercaptoethanol, and 0.01 % bromophenol blue). Samples were immediately heated at 95 °C for 3 min. Equal volumes of samples were run on an SDS-12 % polyacrylamide gel and were transferred to nitrocellulose membrane by semidry transfer at 50 mA for 1 h. Blots were probed with specific antibodies of Caspase 3 (1: 2 000; IMG144A) and tubulin (as loading control) (1:5 000; Sigma #T5168) and stained with anti-mouse (Caspase 3) and anti-rabbit (tubulin) secondary antibody coupled with horseradish peroxidase (Sigma). Bands were visualized using an enhanced chemiluminescence protocol (Pierce) and radiographic film (Kodak). Developed radiographic film was scanned and band intensities were quantified using Image J software ([www.imagej.en.softonic.com](http://www.imagej.en.softonic.com)).

## Statistical analysis

Statistical significance was calculated between the untreated control cells Vs treatments. Data are presented as mean  $\pm$  standard error mean (SEM) and statistical analysis of data was performed by Unpaired-t test using graphpad software ([www.graphpad.com](http://www.graphpad.com)).

## Acknowledgments

Authors gratefully acknowledge financial support from the University Grants Commission, New Delhi and 12th FYP project (AARF, CSC0406) from CSIR, New Delhi, India. Thanks are due to Dr. Nishant S Jain, Chemical Biology Division, IICT, Hyderabad for providing the facility for SRB assay and western blotting. We express our thanks to Prof. T. Papi Reddy, Former Head, Department of Genetics, Osmania University for critical reading of the manuscript. NC and SRB thank UGC, New Delhi for providing research fellowship.

## Conflicts of Interest

Authors declare there are no conflicts of interest.

## References

- [1] Fridlender M, Kapulnik Y, Koltai H. Plant derived substances with anti-cancer activity: from folklore to practice. *Front Plant Sci* 2015; 6: 799
- [2] Chavan SS, Damale MG, Shamkuwar PB, Pawar DP. Traditional medicinal plants for anticancer activity. *Int J Curr Pharm Res* 2013; 5: 50–54
- [3] Abhyankar G, Suprasanna P, Pandey BN, Mishra KP, Rao KV, Reddy VD. Hairy root extract of *Phyllanthus amarus* induces apoptotic cell death in human breast cancer cells. *Innov Food Sci Emerg Technol* 2010; 11: 526–532
- [4] Cherukupalli N, Divate M, Mittapelli SR, Khareedu VR, Vudem DR. De novo assembly of leaf transcriptome in the medicinal plant *Andrographis paniculata*. *Front Plant Sci* 2016; 7: 1203
- [5] Valdiani A, Talei D, Javanmard A, Tan SG, Kadir MA, Maziah M. Morpho-molecular analysis as a prognostic model for repulsive feedback of the medicinal plant "*Andrographis paniculata*" to allogamy. *Gene* 2014; 542: 156–167
- [6] Luo W, Liu Y, Zhang J, Luo X, Lin C, Guo J. Andrographolide inhibits the activation of NF- $\kappa$ B and MMP-9 activity in H3255 lung cancer cells. *Exp Ther Med* 2013; 6: 743–746
- [7] Mishra SK, Tripathi S, Shukla A, Oh SH, Kim HM. Andrographolide and analogues in cancer prevention. *Front Biosci* 2015; 7: 255–266
- [8] Talei D, Valdiani A, Maziah M, Sagineedu SR, Saad MS. Analysis of the anticancer phytochemicals in *Andrographis paniculata* Nees. under salinity stress. *Biomed Res Int* 2013; 2013: 319047
- [9] Sangameswaran B, Ilango K. Evaluation anti-hyperglycemic and anti-hyperlipidaemic activities of *Andrographis lineata* Nees on streptozotocin induced diabetic rats. *Jordan J Biol Sci* 2010; 3: 83–86
- [10] Parlapally S, Cherukupalli N, Bhumireddy SR, Sripadi P, Aniseti R, Giri CC, Khareedu VR, Reddy VD. Chemical profiling and anti-psoriatic activity of methanolic extract of *Andrographis nallamalayana* J.L.Ellis. *Nat Prod Res* 2015; 8: 1–6
- [11] Kandati V, Govardhan P, Reddy CS, Nath AR, Reddy RR. In-vitro and in-vivo anti-inflammatory activity of *Andrographis serpyllifolia* (Rottl. Ex Vahl.) Wt. *Int Curr Pharm J* 2012; 1: 199–204
- [12] Neeraja C, Krishna PH, Reddy CS, Giri CC, Rao KV, Reddy VD. Distribution of *Andrographis* species in different districts of Andhra Pradesh. *Proc Natl Acad Sci India Sect B Biol Sci* 2015; 85: 601–606
- [13] Gupta KK, Bharne SS, Rathinasamy K, Naik NR, Panda D. Dietary antioxidant curcumin inhibits microtubule assembly through tubulin binding. *FEBS J* 2006; 273: 5320–5332
- [14] Jackson SJ, Murphy LL, Venema RC, Singletary KW, Young AJ. Curcumin binds tubulin, induces mitotic catastrophe, and impedes normal endothelial cell proliferation. *Food Chem Toxicol* 2013; 60: 431–438
- [15] Arolla RG, Neeraja C, Rao KV, Reddy VD. DNA barcoding and haplotyping in different species of *Andrographis*. *Biochem Syst Ecol* 2015; 62: 91–97
- [16] Martinez-Perez C, Ward C, Cook G, Mullen P, McPhail D, Harrison DJ. Langdon SP. Novel flavonoids as anti-cancer agents: Mechanisms of action and promise for their potential application in breast cancer. *Biochem Soc Trans* 2014; 42: 1017–1023
- [17] Ravishankar D, Rajora AK, Greco F, Osborn HM. Flavonoids as prospective compounds for anti-cancer therapy. *Int J Biochem Cell Biol* 2013; 45: 2821–2831
- [18] Selvendiran K, Koga H, Ueno T, Yoshida T, Maeyama M, Torimura T, Yano H, Kojiro M, Sata M. Luteolin promotes degradation in signal transducer and activator of transcription 3 in human hepatoma cells: An implication for the antitumor potential of flavonoids. *Cancer Res* 2006; 66: 4826–4834
- [19] Hodek P, Tepla M, Krizkova J, Sulc M, Stiborova M. Modulation of cytochrome P450 enzyme system by selected flavonoids. *Neuro Endocrinol Lett* 2009; 30: 67–71
- [20] Mohammed A, Chiruvella KK, Rao YK, Geethangili M, Raghavan SC, Ghanta RG. In vitro production of echiodinin, 7-O-methywogonin from callus cultures of *Andrographis lineata* and their cytotoxicity on cancer cells. *PLoS One* 2015; 10: e0141154
- [21] Vijayalakshmi A, Masilamani K, Nagarajan E, Ravichandiran V. In vitro antioxidant and anticancer activity of flavonoids from *Cassia tora* Linn. leaves against human breast carcinoma cell lines. *Der Pharma Chemica* 2015; 7: 122–129
- [22] Guo X, Rukiya M, Mourboul A, Sheng L, Abulizi A. Anti-cancer activity of flavonoids from *Xinjiang Glycyrrhiza inflata* Licorice on proliferation, cytotoxicity and apoptosis in cervical carcinoma cells. *J Med Plant Res* 2013; 7: 173–188
- [23] Park KI, Park HS, Nagappan A, Hong GE, Lee do H, Kang SR, Kim JA, Zhang J, Kim EH, Lee WS, Shin SC, HahYS Kim GS. Induction of the cell cycle arrest and apoptosis by flavonoids isolated from Korean *Citrus aurantium* L. in non-small-cell lung cancer cells. *Food Chem* 2012; 135: 2728–2735
- [24] Yamaguchi M, Murata T, El-Rayes BF, Shoji M. The flavonoid p-hydroxycinnamic acid exhibits anticancer effects in human pancreatic cancer MIA PaCa-2 cells in vitro: Comparison with gemcitabine. *Oncol Rep* 2015; 34: 3304–3310
- [25] Mojzis J, Varinska L, Mojzisova G, Kostova I, Mirossay L. Anti-angiogenic effects of flavonoids and chalcones. *Pharmacol Res* 2008; 57: 259–265
- [26] Wang L, Wang J, Fang L, Zheng Z, Zhi D, Wang S, Li S, Ho CT, Zhao H. Anticancer activities of citrus peel polymethoxyflavones related to angiogenesis and others. *Biomed Res Int* 2014; 453972
- [27] Elumalai N, Ayyakkannu P, Palanivelu S, Panchanadham S. In vitro antioxidant potential of *Shemamruthaa* (a herbal formulation) and its anticancer activity in the MCF-7 cell line. *RSC Adv* 2015; 5: 23125–23133
- [28] Carini JP, Klamt F, Bassani VL. Flavonoids from *Achyrocline satureioides*: Promising biomolecules for anticancer therapy. *RSC Adv* 2014; 4: 3131–3144
- [29] Desagher S, Martinou JC. Mitochondria as the central control point of apoptosis. *Trends Cell Biol* 2000; 10: 369–377

- [30] Zamzami N, Susin SA, Marchetti P, Hirsch T, Gómez Monterrey I, Castedo M, Kroemer G. Mitochondrial control of nuclear apoptosis. *J Exp Med* 1996; 183: 1533–1544
- [31] Li PD, Nijhawan D, Budihardjo I, Srinivasula SM, Ahmad M, Alnemri ES, Wang X. Cytochrome c and dATP-dependent formation of Apaf-1/caspase 9 complex initiates an apoptotic protease cascade. *Cell* 1997; 91: 479–489
- [32] Green DR, Reed JC. Mitochondria and apoptosis. *Science* 1998; 281: 1309–1312
- [33] Shi Y. A structural view of mitochondria-mediated apoptosis. *Nat Struct Biol* 2001; 8: 394–401
- [34] McIlwain DR, Berger T, Mak TW. Caspase functions in cell death and disease. *Cold Spring Harb Perspect Biol* 2015; 7: a026716